

# New Application of Nested Sequential Forward Feature Selection: Optimizing Instrumental Odour Monitoring Systems in Drones

Javier Alonso-Valdesueiro<sup>a</sup>, Alessandro Benegiamo<sup>b</sup>, Javier Burgues<sup>a</sup>, Albert Vidal<sup>b</sup>, Agustin Gutierrez-Galvez<sup>a</sup>, Santiago Marco<sup>a,b</sup>

<sup>a</sup>Department of Electronic and Biomedical Engineering, University of Barcelona, Martí i Franquès 1., Barcelona, 08028, Catalonia, Spain

<sup>b</sup>Signal and Information Processing for Sensing Systems Group, Institute for Bioengineering of Catalonia, Baldri i Reixac, 4 Torre I, Barcelona, 08028, Catalonia, Spain

---

## Abstract

This study aims to present a new application of the Nested Sequential Forward Feature Selection algorithm when applying to optimize the performance of Instrumental Odour Monitoring Systems on-boarded in drones. When combined with The Interval Partial Least Square Regression model (the NiPLS algorithm), it reduces the Root Mean Square error of prediction (RMSEP) and the Limits of Agreement (LoA) at 95% Confident Interval (CI) compared with traditional approaches in Feature selection and Cross Validation of the model. The algorithm is applied twice, first for selecting the most relevant sensors and then, for selecting the most relevant period of acquisition. This optimization procedure was tested on data obtained from the IOMS onboarded in an octocopter drone flying over a Waste Water Treatment Plant (WWTP). The RMSEP reduced from 2.1x to 1.8x and maximum LoA at 95% CI reduces from 5x to 3.4x with correlation coefficient of 0.9 when measurements were taken from different sources in a particular WWTP.

**Keywords:** Instrumental Odour Monitoring System, Chemical sensors, Feature selection, Odour quantification, On-boarded system, Drone Instrumentation

---

## 1. Introduction

Odour quantification in industrial environments have recently attracted attention due to legal regulation in modern countries [1, 2, 3]. Governments have established regulation on measurement methods and permitted levels of odour in different situations [4]. The most extended method for odour quantification is the dynamic olfactometry, where a human panel determines the level of odour when exposed to a sample of air [5]. The air is taken from the industrial environment under study in sampling bags, diluted at different concentrations and delivered to the human panel for quantifications. Despite its extended use and legal endorsement, odour quantification using dynamic olfactometry presents several problems that reduces its applicability. First, it presents a Limit of Agreement (LoA) of 2x with a Confident Interval (CI) of 95% in every quantification [ref]. Second, it only allows punctual pool of the industrial environment. And finally, a full characterization of the odour coming from an industrial plant might scale in budget quite fast.

For these reasons, in the last decades, Instrumental Our Monitoring Systems (IOMSs) have been deployed as odour quantification tools in industrial environments [6]. In particular, their deployment in Wastewater Treatment Plants (WWTPs) have demonstrated to be a very useful tool for plant managers regarding adjust the odour levels to the legal regulation [7]. Furthermore, new designs which consist in on-boarded IOMS in drones, have been developed aiming 3D odour maps of WWTPs [8, 9]. When the IOMS is flying in a drone, the cost reduction by using IOMSs instead of odour characterization campaigns by dynamic olfactometries, reduces even further. Within two days campaign, a characterization relevant odour emitters and a 3D odour map can be provided. Even, the odour quantification can be dynamically monitored, allowing the operator to choose where and when to sample.

The on-boarded IOMS is typically equipped with an array of chemical sensors of different types and takes off with the drone. Flying over different odour sources in the plant, the IOMS measures the concentration of different gases in the air while sampling bags are filled.

Once the measurements are done, dynamic olfactometries are performed using the sampling bags and an odour level in  $OU_E/m^3$  is provided for each source of the plant [8, 10, 9]. Therefore, each source is represented by a temporal series of measurements (one temporal series per sensor) or features and an odour level. With this information, the IOMS is calibrated using multivariate prediction models. The models are trained with the data from the sensor array and the dynamic olfactometries and, afterwards, the model quantifies the odour by observing the signals coming from the sensor array.

Partial Least Squares (PLS) [11] is the most common multivariate model to predict odour concentration in the field [7, 10]. Particularly well suited for datasets with time series and few samples, its performance can be improved by reducing the features in each sample by different reduction methods. In the field of on-boarded IOMSs, the Variable Importance in Projection (VIP) method [12] has become the most extended feature reduction method.

In this method, VIPs scores are calculated as the squares of the PLS weights provide information of the explained variance associated to each latent variable. Features with VIPs are selected following the “greater than one” rule for model optimisations, where a VIP score above 1 keeps the feature for future model training. Then, different techniques are applied for further elimination of data from the training dataset []. After this selection of features, the leave-one-block-out Cross Validation (CV) scheme [13] is commonly used for validation looking at the Root Mean Square Error of Cross Validation (RMSECV).

This procedure typically leads to RMSEP in the quantification of odour 2.3x which in the worst-case scenario becomes a Limit of Agreement of 5x with 95% CI []. Therefore, the advantages of using on-boarded IOMSs in industrial plants get downsized by this poor performance and leave their use out of legal quality assessment or regulatory studies of the plants. In the last decade, a considerable amount of effort has been put on reduce the RMSEP of the model after CV by applying new algorithms able to work with datasets with small number of samples [14, 15, 16, 17].

It is the aim of this contribution to present a new approach to this problem. Working with a small dataset obtained by an IOMS on-boarded in an DJI drone when flying over odour sources in a WWTP, the proposed solution is able to reduce the RMSEP and downsize the LoA at 95% of CI by two points. A two step process for feature selection, based on the knowledge of the characteristics of the data collected by the IOMS, is presented. It uses a Nested Sequential Forward Selection

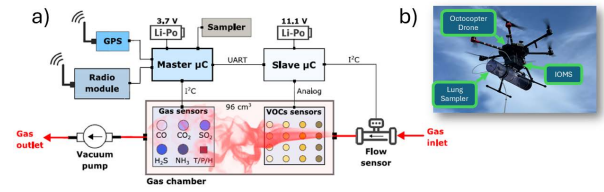


Figure 1: IOMS onboarded in the flying drone. (a) Block Diagram of the onboarded IOMS. The drawing includes the communications modules, the lung sampler and the batteries. (b) Onboarded Hardware in the DJI octocopter. The figure shows the drone, the IOMS and the lung sampler.

algorithm [18, 19] in combination with Interval Partial Least Squares procedure [20]. The process is applied twice, first for selecting the most relevant sensors and then, for selecting the most relevant period of acquisition.

The presented contribution is organized as follows. Firstly, in the Methods section, the onboarded IOMS and the measurements campaign are presented. Also in this section, the data processing workflow is described with detail. Secondly, in the Results and Discussion section, the performance figures of the proposed workflow are summarized when applied to the dataset obtained in the measurement campaign. Finally, in the Conclusions section, a summary of the NiPLS performance is presented and its future applications in the field of on-boarded IOMSs are described.

## 2. Methods

### 2.1. Onboarded IOMS

Fig.1(a) shows the block diagram of the onboarded IOMS performing measurements during flights.

The IOMS consists of a Gas Chamber with 5 electrochemical sensors and 16 MOX sensors in a 96 cm<sup>3</sup> volume, all listed in tables 1 and 2. All the electrochemical sensors were bought from Alphasense Inc. and they are interfaced with a microcontroller from Libellium via proprietary Analog Frontends. The MOX sensors belong to the TGS series from Figaro. As is described in Table 1, series of TGS2600, TGS2602, TGS2611 and TGS2620 are heated up by applying different voltages using PWM signals, which lead to different temperatures [21, 22]. The PWM signals are produced by an Arduino device and conditioned for power transfer by a custom-made electronic platform.

Fig.1(b) shows all the equipment onboarded in a DJI octocopter when flying. It includes the IOMS and the lung sampler used for collecting sample-bags filled with environmental air. Both, the IOMS and the lung sampler

	Technology	Range	Accuracy	Resp. time (T <sub>90</sub> )
Flow rate	Ultrasonic	-33 to +33 L/min	±3% m.v.	<1 s
CO <sub>2</sub>	NDIR	0 to 5000 ppm	±100 ppm	<60 s
CO	Electrochemical	0 to 100 ppm	±0.5 ppm	<20 s
H <sub>2</sub> S	Electrochemical	0 to 20 ppm	±0.1 ppm	<20 s
NH <sub>3</sub>	Electrochemical	0 to 100 ppm	±0.5 ppm	<90 s
SO <sub>2</sub>	Electrochemical	0 to 20 ppm	±0.1 ppm	<45 s

Table 1: Specifications of electrochemical, NDIR and Flow sensor

Sensor	Model	Target gases	Heater voltage (V)
M1,2,3,4	TGS 2600	H <sub>2</sub> , CO, Ethanol	1.6,3,2,4,0,4,9
M5,6,7,8	TGS 2602	H <sub>2</sub> S, NH <sub>3</sub> , Toluene	1.6,3,2,4,0,4,9
M9,10,11,12	TGS 2611	CH <sub>4</sub> , Hydrocarbons	1.6,3,2,4,0,4,9
M13,14,15,16	TGS 2620	Alcohols, ketones	1.6,3,2,4,0,4,2

Table 2: Specifications of the MOX sensors included in the slave board

have a 10 meters PTFE tube connected to their input. This distance is more than enough for avoiding down washing effect from the drone [23, 24]. The tubes collect air from the same environment when the drone is flying over the plant.

The air is sucked with a Vacuum pump and the airflow is measured with a flow sensor also described in table 1. Every data produced by the sensors (electrochemical, MOX and flow sensor) is collected by the Libellium microcontroller and, among battery data, gps location data and other status data, is framed and sent via an Xbee module to a groundbased laptop.

The laptop runs a custom-made software that collects the data sent by the IOMS via Xbee, record it and plots the results on the screen. The software also allows the user to command the IOMS to activate the lung sampler, making the readings from the sensors synchronized with the air filling the bug inside the lung sampler. Bags are usually collected at different locations in the WWTP and transported to a certified company which perform dynamic olfactometric analysis with the air inside the bags. Once the odour quantification is provided by the company, the data recorded from the sensors at each location and the odour quantification in  $OU_E/m^3$  are used to calibrate a odour prediction model. For more information about the IOMS consult previous work [8, 10]

## 2.2. Measurement Campaign

Fig.2 shows the WWTP where the measurement campaign was performed. It is located in the south-west of Spain and presents a typical topology of a WWTP.

The major contribution on the odour level at each source is the combination of the gases emitted by the source itself [7]. Environmental factors (wind, temperature, humidity) have also influence in the odour level

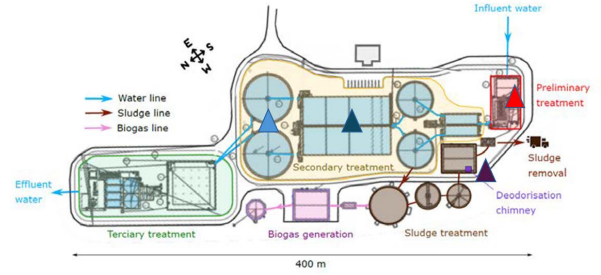


Figure 2: Waste Water Treatment Plant where the measurement campaign was performed. ▲ Primary Settler, ▲ Bioreactor, ▲ Preliminary Treatment Building, ▲ Deodorisation Chimney.

Day	Date	Settler▲	Bioreactor▲	Pretreatment▲	Chimney▲	Total (odour)	Blanks	Total
1	24/06/2020	3	3	2	2	10	7	17
2	25/06/2020	2	2	2	2	8	6	14
3	14/07/2020	3	3	3	3	12	11	23
4	15/07/2020	3	3	3	3	12	7	19
Total		11	11	10	10	42	31	73

Table 3: Number of samples collected in each source during the four measurement days

but under the same conditions, it is the source emission which determines the odour level when performing dynamic olfactometries [25]. The Primary Settler (▲ in Fig.2) is typically a source of xxxx and the Bioreactor and the Preliminary Treatment Building (▲ and ▲ in Fig.2) are typically sources of xxxx. Finally, the Deodorisation Chimney (▲ in Fig.2) is usually a source of xxxx.

The campaign consisted in 4 days of measurements with the drone flying over the 4 sources. Table 3 summarizes the measurements. Each day at least two bags were collected at each source, each of them at different heights. Also, locations where the odour level was low (called blanks in Table 3) were sampled. Fig.3 shows the readings from the different sensors obtained in the first day of the measurement campaign. For more information about the IOMS consult previous work [8, 10]

## 2.3. General Workflow

The data analysis performed to produce an odour level prediction model is depicted in Fig.4(a). In this figure, a general overview of the training and validation process is presented accordingly with previous publications [8, 9, 10].

Firstly, the sensor readings are pre-processed using different techniques for MOX sensors and Electrochemical sensors. A log-transformation was applied at every data sequence recorded with the IOMS. The Feature matrix was organized forming a total matrix of  $n \times m$  rows and columns, where each row corresponds to a

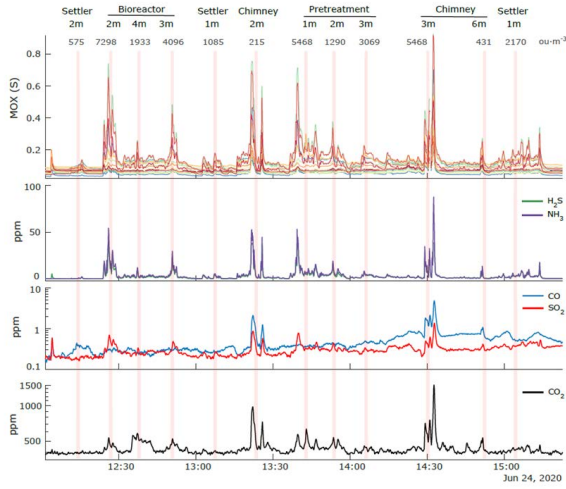


Figure 3: Sensor readings in the first day of campaign. The figure includes the response of the 16 MOX sensors, the H<sub>2</sub>S and the NH<sub>3</sub> sensors, the CO and the SO<sub>2</sub> sensors, and the CO<sub>2</sub> sensor. The vertical pink bars indicate the moment when the lung sampler was on.

sampling bag collected with the lung sampler and each column to a single value of the sensor readings.

The vertical lines at Fig.3 mark when the lung sampler is activated. Around this marks, 5 minutes are considered as relevant for the analysis. The rest of the time series is removed from the features. In total the feature matrix has dimensions of 73x945 including blanks for pre-processing purposes (73 samples by 21 sensors multiplied by 45 *samples/sensor*). After using the blanks and leaving not-useful samples out of the matrix, the final feature matrix consists in 40x945 matrix where each sensor has 45 features at each sample.

After building the feature matrix, a Partial Least Squares model is built as explained in [15]. The Variable Importance Projection (VIP) method is first applied for feature extraction, leaving out features with VIP scores <1. The VIPs of each sensor are averaged per day at every feature (45 per sample for each sensor), leading to an averaged VIP score distribution depicted in Fig. 6 (b). Then, a double leave-one-block-out cross-validation (CV) scheme is performed for model building. This scheme takes three days for model training and leaves out one day for validation and produces 4 different models.

In order to avoid complexity grow uncontrolled at each of the proposed models, within each calibration set the “leave one sample out” (LOO) scheme is used. N PLS models are built with different Latent Variables (LVs) leaving a sample for test out of the building process. The number of LVs is therefore optimized by eval-

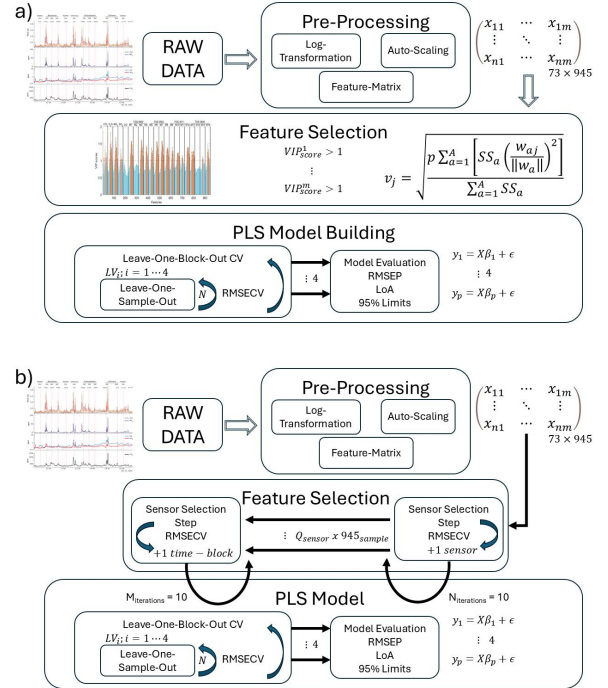


Figure 4: Data analysis Workflow. (a) General Workflow with Feature Selection based on VIP calculation and discrimination. (b) Modified Workflow with NiPLS as Feature Selection methodology.

uating the Root Mean Square Error in Cross Validation (RMSECV). Finally, the models are refit using the calibration samples used during training and used to produce prediction plots on blind samples. The bias of the prediction and 95% limits of agreement (LoA) are computed using the Bland-Altman methodology [26].

#### 2.4. Nested Sequential Forward Selector using iPLS for Odour Quantification

The presented workflow is optimal for dataset with low number of samples. In the performed measurement campaign this number reduces to 73 where almost half of the samples correspond to blank samples used for signal correction. Its strength is based in the Cross Validation technique that performs Leave-one Block-Out and Leave-one Sample-Out nested to get optimized models. However, the feature selection is performed using a more general procedure and it does not take into account the peculiarities of the acquired dataset.

Fig.4(b) shows the modified data analysis workflow proposed to optimize the feature selection stage of the workflow presented in subsection 2.3 and depicted in Fig.4(a).

The methodology is very similar to the methodology applied for CV but it consists of two steps. First, a PLS model is built using the general workflow but including only one sensor of the sequence of 945 features of each sample. The RMSECV is calculated and then the another PLS model is built including a different sensor. The process is iterated until a minimum in the RMSECV is observed. In this case, the minimum was clear after 10 iterations. As depicted in Fig.8(a), at each iteration, the presented table provides information about which sensors are included in the feature matrix (■) and which are not (■).

After this optimization, at each sample, the information of the most relevant sensors is included in the feature matrix. Then, the time-slot of each sensor (the 5 minutes window corresponding to the pink vertical bar in Fig.3) is divided in 15 blocks, which corresponds to time-blocks of 20 seconds. With this partition, a similar procedure than the one described in the Sensor step is performed. Time-blocks are added to the model building process and the RMSECV is observed. After 10 iterations a minimum appears to be clear for a selection of time-blocks.

This method reduces considerable the complexity of the feature matrix and the noise associated to non-consequent sensors and time-blocks of each sensors. This leads to more general models that perform better in the test stage.

### 3. Results and Discussion

#### 3.1. Gas Concentration Measurements

Fig. 3 shows the an example of data collected by the IOMS during a day of campaign. Data collected from the different sensors is pre-processed using the different blanc samples and baseline level is corrected with the lowest value of the day recorded for each sensor. After this adjustment, the 5 minutes time-slot around the sampling bag filling (■ rectangle in Fig. 3, which correspond to 45 samples) is placed in the feature matrix as explained in Fig. 4. The feture matix is then pre-processed according to the general workflow and the result is depicted in Fig. 5.

A more detailed analysis is presented in Fig. 6. In this figure, the data from the H<sub>2</sub>S and NH<sub>3</sub> sensors is depicted with the 5 minute time-slot which correspond to the data included in the feature matrix (see Fig. 6 (a)).

Fig. 6 (b) shows the VIP for each sensor averaged at each day. The VIP analysis shows that inside this 5 minute-slot the most relevant features are commonly

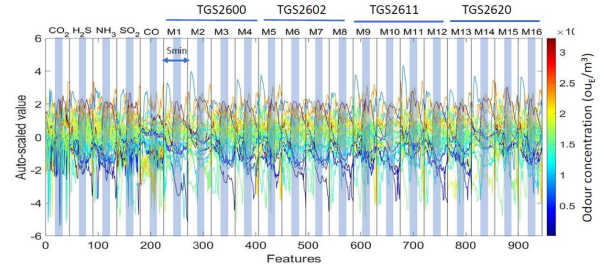


Figure 5: Preprocessed data of the different sources for every day of the measurement campaign. The 5 minutes of valid data have been marked in the plot.

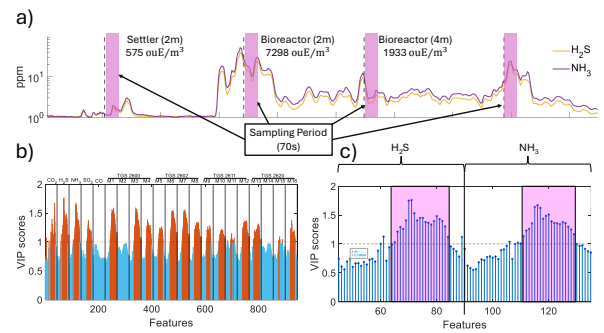


Figure 6: Detail of the signal acquired from two of the most significant sensors (H<sub>2</sub>S and NH<sub>3</sub>) when the drone is flying over several sources and VIP scores. (a) Detail of the signal acquired and sampling period (■). (b) Distribution of the VIP scores of every sensor when averaged over the four days of campaign at every time-slot. (c) Detail of the averaged VIP scores for H<sub>2</sub>S and NH<sub>3</sub>. The sampling period is also marked (■).

placed at the end of the sampling bag filling processed. In particular, there are 21 samples which produce VIPs > 1, which reduces the relevant samples further more. Also it is observed that the higher values for the VIP scores belong to the H<sub>2</sub>S and NH<sub>3</sub> electrochemical sensors and some of the MOX sensors.

Therefore, it should be possible to reduce further more the features used to train the prediction PLSR model by selecting the sensor and the features of each sensor in the 5 minute time-slot.

#### 3.2. General Workflow Performance

In orther to compare the performance of the NiPLS workflow with workflows presented in the literature [10, 9] the performance of the workflow depicted in Fig. 4 (a) is presented in Fig. 7.

In this case, when 40 samples are considered (from the 73 acquired and after removing blanks) the best PLRS model presente 2 Latent Variables. This model obtains an RMSEP of 2.13x for 4 sources considered at



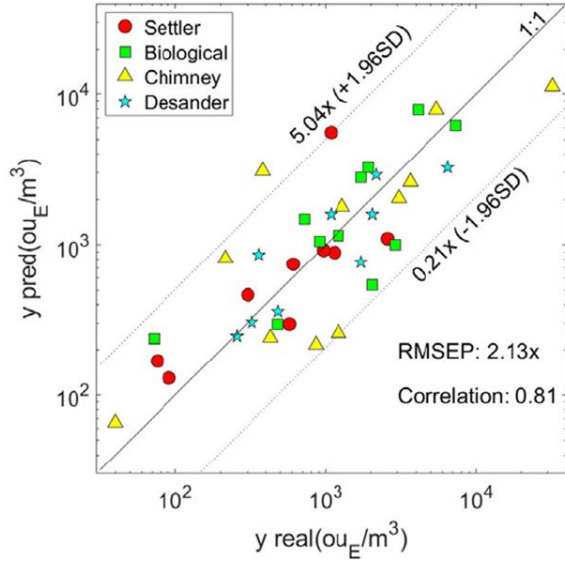


Figure 7: Performance of the general workflow presented in section 2.3. The number of useful samples have been reduced to 40 plus blanks. Prediction plot for the best PLS model built with LoA limits at 95% CI of  $[0.2x - 5.0x]$  and correlation coefficient of 0.81.

different heights, the Settler ( $\Delta$ ), the Bioreactor ( $\Delta$ ), the Chimney ( $\Delta$ ) and the Pretreatment Building ( $\Delta$ ). In this case the calculated LoA at 95% CI lies in the  $0.2x$  to  $5x$  range of the prediction

### 3.3. NiPLS Performance

With the NiPLS presented in Fig. 4 (b) the results of the novel feature selection algorithm are presented. When the iPLS achieves the fourth iteration the RMSECV goes down in both steps of the selection process (sensor step and time-slot step).

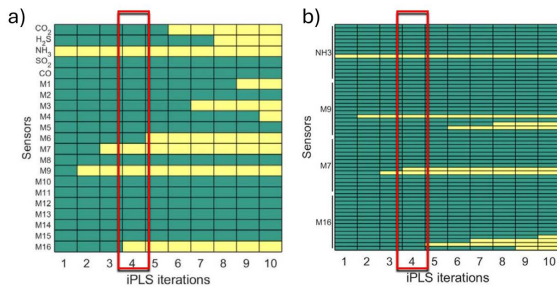


Figure 8: Nested Sequential Forward Selector.  $\square$  interval included in the feature matrix,  $\square$  interval not included in the feature matrix (a) Sensor Step. (b) Time-slot Step.

In the sensor step, four sensors are selected as most relevant. The  $\text{NH}_3$  from the electrochemical sensors and the MOX sensors M7, M9 and M16. These

MOX sensors belong to the second (TGS26002), third (TGS2611) and fourth (TGS2620) group of MOX sensors (see Table 2) at 4.0 V, 1.6 V and 4.2 V respectively.

In the time-slot step, 4 time-slot of the preselected sensors are selected as the most relevant features of these sensors. However, in this case the, features from the MOX sensors M16 (TGS2620 at 4.2 V) are left out. For the  $\text{NH}_3$ , M7 and M9 sensors, the selected features correspond to the central part of the 45 features.

With this features, the resulted PLSR model shows the performance depicted in Fig. 9

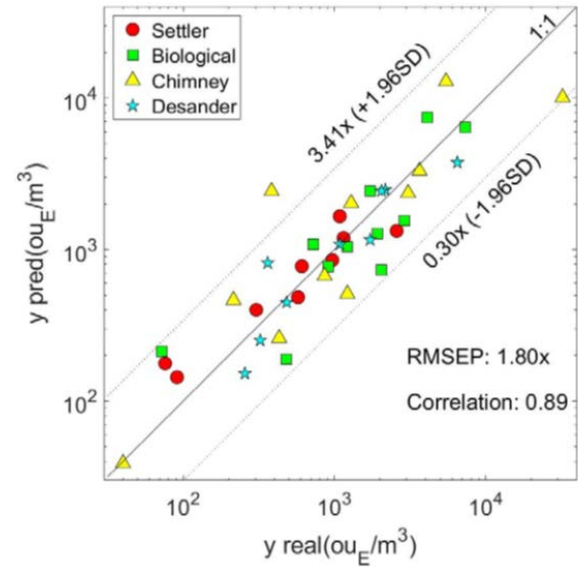


Figure 9: Performance of the optimized model using NiPLS. The number of useful samples have been reduced to 40 plus blanks. The model shows LoA limits at 95% CI of  $[0.3x - 3.4x]$  and a correlation coefficient of 0.89.

A reduction of the RMSEP is observed when the same set of samples used in Section 3.2 is considered. The NiPLS model shows a RMSEP of  $1.8x$  and the LoA at 95% CI lies in the  $0.3x$  to  $3.4x$  range, which is a considerable improvement when traditional feature selection is applied to the data set (see Fig. 7).

## 4. Conclusions

In this contribution, a novel application of the Nested Sequential Forward Feature Selection algorithm is presented. Its combination with the Interval Partial Least Square Regression model, when modified accordingly for the special case of IOMSs studding odour concentrations in Waste Water Treatment Plants, proves to improve the performance of the model comparing with traditional approaches. In particular, for the measurement

campaign performed in a WWTP in Spain, the novel workflow shows an improvement on the RMSEP of 0.2 point and a reduction of the Limit of Agreement at 95% CI from 5x to 3.4x.

These results enhance the performance of IOMS onboarded in drones evaluating odour emission and allows to use it as a complementary odour analysis tool to the dynamic olfactometry in WWTPs.

Furthermore, the novel workflow shows relevant information when considering improvement on the IOMS. The information of the relevant sensors might be used to reduce the size and the data load transferred from the IOMS to the ground PC.

## References

- [1] T. Brinkmann, R. Both, B. Scalet, S. Roudier, L. Sancho, Jr reference report on monitoring of emissions to air and water from industrial installations, EUR 29261 EN. Eur. IPPC Bur. Eur. Comm. Jt. Res. Cent. (2018).
- [2] T. Group, Integrating climate into our strategy [www document], [https://www.total.com/sites/default/files/atoms/files/total\\_rapport\\_climat\\_2019\\_en](https://www.total.com/sites/default/files/atoms/files/total_rapport_climat_2019_en). (2019).
- [3] F. Zhou, S. Pan, W. Chen, X. Ni, B. An, Monitoring of compliance with fuel sulfur content regulations through unmanned aerial vehicle (uav) measurements of ship emissions, *Atmos. Meas. Tech.* 12 (2019).
- [4] Scentroid, Eu police using scentroid dr1000 flying lab to combat smog [www document], [http://scentroid.com/police\\_using\\_scentroid\\_dr1000\\_flying\\_lab\\_tocombat\\_smog/](http://scentroid.com/police_using_scentroid_dr1000_flying_lab_tocombat_smog/) (2018).
- [5] S. Sironi, L. Capelli, P. Céntola, R. Del Rosso, S. Pierucci, Odour impact assessment by means of dynamic olfactometry, dispersion modelling and social participation, *Atmospheric Environment* 44 (3) (2010) 354–360.
- [6] F. Cangialosi, G. Intini, D. Colucci, On line monitoring of odour nuisance at a sanitary landfill for non-hazardous waste, *Chem. Eng. Trans* 68 (2018) 127–132.
- [7] L. Capelli, S. Sironi, P. Céntola, R. Del Rosso, M. Grande, Electronic noses for the continuous monitoring of odours from a wastewater treatment plant at specific receptors: Focus on training methods, *Sensors and Actuators B: Chemical* 131 (1) (2008) 53–62, special Issue: Selected Papers from the 12th International Symposium on Olfaction and Electronic Noses.
- [8] J. Burgués, S. Marco, Environmental chemical sensing using small drones: A review, *Science of The Total Environment* 748 (2020) 141172.
- [9] J. Burgués, M. D. Esclapez, S. Doñate, L. Pastor, S. Marco, Aerial mapping of odorous gases in a wastewater treatment plant using a small drone, *Remote Sensing* 13 (9) (2021).
- [10] J. Burgués, M. D. Esclapez, S. Doñate, S. Marco, Rhinos: A lightweight portable electronic nose for real-time odor quantification in wastewater treatment plants, *iScience* 24 (12) (2021) 103371.
- [11] S. Wold, A. Ruhe, H. Wold, W. J. Dunn, III, The collinearity problem in linear regression. the partial least squares (pls) approach to generalized inverses, *SIAM Journal on Scientific and Statistical Computing* 5 (3) (1984) 735–743.
- [12] I. Chong, J. C.H., Performance of some variable selection methods when multicollinearity is present, *Chemometrics and Intelligent Laboratory Systems* 78 (1) (2005) 103–112.
- [13] P. Filzmoser, B. Liebmann, K. Varmuza, Repeated double cross validation, *Journal of Chemometrics* 23 (4) (2009) 160–171.
- [14] T. Hastie, R. Tibshirani, J. Friedman, *The Elements of Statistical Learning: Data Mining, Inference, and Prediction*, 2nd Edition, Springer, New York, 2009.
- [15] S. Wold, M. Sjöström, L. Eriksson, Pls-regression: A basic tool of chemometrics, *Chemometrics and Intelligent Laboratory Systems* 58 (2) (2001) 109–130.
- [16] H. Martens, T. Naes, *Multivariate Calibration*, John Wiley & Sons, Chichester, 1989.
- [17] S. Arlot, A. Celisse, A survey of cross-validation procedures for model selection, *Statistics Surveys* 4 (2010) 40–79.
- [18] A. K. Jain, D. Zongker, Feature selection: Evaluation, application, and small sample performance, *IEEE Transactions on Pattern Analysis and Machine Intelligence* 19 (2) (1997) 153–158.
- [19] Y. Saey, I. Inza, P. Larrañaga, A review of feature selection techniques in bioinformatics, *Bioinformatics* 23 (19) (2007) 2507–2517.
- [20] L. Nørgaard, A. Saudland, J. Wagner, J. P. Nielsen, L. Munck, S. B. Engelsen, Interval partial least-squares regression (ipls): A comparative chemometric study with an example from near-infrared spectroscopy, *Applied Spectroscopy* 54 (3) (2000) 413–419.
- [21] J. Fonollosa, L. Fernández, R. Huerta, A. Gutiérrez-Gálvez, S. Marco, Temperature optimization of metal oxide sensor arrays using mutual information, *Sensors and Actuators B: Chemical* 187 (2013) 331–339, selected Papers from the 14th International Meeting on Chemical Sensors.
- [22] J. Burgués, S. Marco, Low power operation of temperature-modulated metal oxide semiconductor gas sensors, *Sensors* 18 (2) (2018) 339.
- [23] Y. Zheng, S. Yang, X. Liu, J. Wang, T. Norton, J. Chen, Y. Tan, The computational fluid dynamic modeling of downwash flow field for a six-rotor uav, *Frontiers of Agricultural Science and Engineering* 5 (2) (2018) 159.
- [24] Y. Zhu, Q. Guo, Y. Tang, X. Zhu, Y. He, H. Huang, S. Luo, Cfd simulation and measurement of the downwash airflow of a quadrotor plant protection uav during operation, *Computers and Electronics in Agriculture* 201 (2022) 107286.
- [25] J. L. Campos, D. Valenzuela-Heredia, A. Pedrouso, A. Val del Río, M. Belmonte, A. Mosquera-Corral, Greenhouse gases emissions from wastewater treatment plants: Minimization, treatment, and prevention, *Journal of Chemistry* 2016 (1) (2016) 3796352.
- [26] P. Taffé, When can the bland & altman limits of agreement method be used and when it should not be used, *Journal of Clinical Epidemiology* 137 (2021) 176–181.